CHEMICAL ENGINEERING TRANSACTIONS
VOL. 73, 2019
A publication of AIDIC
The Italian Association of Chemical Engineering
Online at www.aidic.it/cet
Guest Editors: Andrea D'Anna, Paolo Ciambelli, Carmelo Sunseri

ISBN 978-88-95608-70-9; **ISSN** 2283-9216
DOI: 10.3303/CET1973012

On the Operation of T-mixer Chemical Reactors in the Cavitation Regime

Khaled Oualha, Mounir Ben Amar, Jean-Philipe Passarello, Andrei Kanaev

Laboratoire des Sciences des Procédés et des Matériaux, CNRS, Université Paris 13, Sorbonne Paris Cité, 99 avenue J.-B. Clément, 93430, Villetaneuse, France
mounir.benamar@lspm.cnrs.fr

The apparition of the cavitation phenomenon in chemical precipitation reactors with rapid micromixing can significantly affect the elaboration process. The bubbles appear in the reactive fluid flow when the local hydrostatic pressure decreases down to the liquid vapour pressure, which also corresponds to the maximum energy input producing the micromixing. In this paper, we study the bubbles kinetics (trajectory, size and number density evolution along the outlet leg of our exocentric T-mixer) in water experimentally by light scattering SLS/DLS measurements and numerically via FLUENT software using the cavitation and population balance models. We conclude about the generation and oscillatory movement of cavitation bubbles with the most abundant sizes between 0.1 and 1 μm, which control allows exploring the cavitation regime of the reactors.
Keywords: T-mixer, Cavitation, Light scattering (DLS/SLS), FLUENT modelling.

1. Introduction

Cavitation plays an important role in chemical engineering processes. It allows activating chemical reactions by a local temperature increase for water purification (Jyoti et al., 2004, Dular et al., 2016) and may affect the size and the polydispersity of nanoparticles elaborated by the sol-gel method (Azouani et al., 2010). The occurrence of this phenomenon in the T-mixture (Oualha et al., 2017a; ibid. 2017b) consumes a significant part of the turbulent energy input directed to the micromixing that alters the process kinetics. However, studies of the related regime of chemical reactors with ultra-rapid micromixing is still missing in literature.
The dynamics of bubbles resulting from cavitation in a biphasic flow have been extensively studied in the past (Lauterborn et al., 1975, Ye et al., 2015, Xiong et al., 2015). Several methods have been applied to the analysis of cavitation bubbles, including laser Doppler anemometry (Huisman et al., 2012), phase Doppler anemometry (Liu et al., 2010) and particle image velocimetry (Shokri et al., 2017).
In this study, we apply experimental laser techniques SLS (static light scattering) and DLS (dynamic light scattering) to analyse the bubbles kinetics in a T-mixer reactor.

2. Experimental Setup

In order to characterize the bubbles and their dynamics inside the T-mixer, we have assembled a new experimental device. The schema of the device is shown in Figure 1a. The water inlet is provided by an adjustable flow meter (Conrad) operating in the range of 0.1-10 l/min. The water input splits into two branches with equal flow rates before being injected into the inlet arms of a T-mixer of a Hartridge-Roughton type depicted in Figure 1b. These inlet arms have equal inner diameters of d_{in} = 1 mm and the outlet tube has the diameter of d_{out} = 2 mm in order to conserve Reynolds number of the fluid (Re_{in}=Re_{out}) according to:

$$Re=4Q\rho k_B T/\mu\pi d \quad (1)$$

Where Q, ρ and μ are flow rate, density and dynamic viscosity of the flow, k_B is Boltzman constant and T is the fluid temperature. The T-mixer is made of transparent material (glass) which allows optical measurements of

Paper Received: 18 May 2018; Revised: 30 July 2018; Accepted: 17 January 2019

Please cite this article as: Oualha K., Ben Amar M., Passarello J.-P., Kanaev A., 2019, On the Operation of T-mixer Chemical Reactors in the Cavitation Regime , Chemical Engineering Transactions, 73, 67-72 DOI:10.3303/CET1973012

the fluid flow. The device is mounted on millimetric displacement stages, which allow measurements at different distances along the outlet tube (z-axis) of the T-mixer at different flow rates of the liquid injection. All experiments were conducted at room temperature of 20 °C.
The light scattering measurements were performed using a single frequency 40 mW / 640 nm Cube 640-40 Circular (Coherent) laser using two monomode optical fibers placed very close to the exit tube surface. One (emitting) fiber transmits the light from the laser to the sample and another receives the photons scattered at right angles to the incident light for analysis. The analysis of the measured light was carried out with a digital 255 channels photon correlator (PhotoCor Instruments). The size of the particles (2R, nm) and the intensity of the scattered light (I, Hz) were measured along z-axis of the T-mixer using respectively the DLS (dynamic light scattering) and SLS (Static light scattering). The measurements were performed in automatic sampling mode with a data storage period of 60 s.

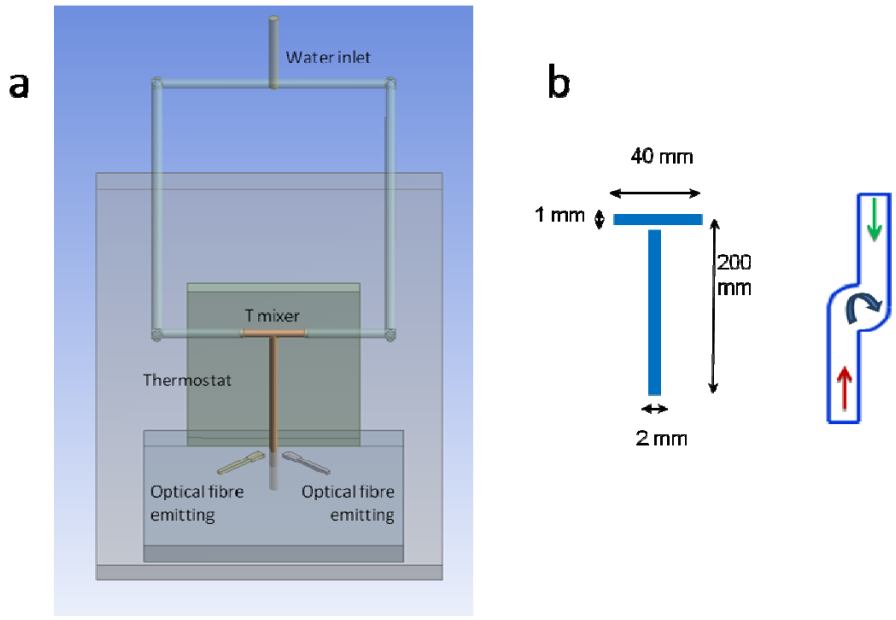

Figure 1: Schema of experimental device (a) and T-mixer (b).

3. Results and discussion

The results of SLS measurement along z-axis of outlet leg of the T-mixer are shown in Figure 2 for fluid flow rates above the cavitation threshold of Q^*=0.75 l/min (Re^*=8000) (Oualha et al., 2017b). The scattering light intensity underwent a general trend to decrease along z-axis distance after the mixing point (z=0) of two inlet flows, exerting in the same time an oscillatory behaviour. Since laser light scattering is produced on the medium inhomogeneities related to the vapour-liquid interface of cavitation, we tentatively explain this general attenuation of intensity by a decrease of the vapour-liquid interface area. This area decrease may be due to the relaxation phenomena consisting in a decrease of the bubbles number and/or size.
On the other hand, the oscillatory variation of the scattered light intensity cannot be explained by the cavitation bubble collapse. We relate this behaviour to the bubbles motion. Indeed, helical trajectories of the fluid inside the T-mixer were experimentally observed as shown in Figure 3a and confirmed by computational fluid dynamics (CFD) simulations shown in Figure 3b. The simulation was performed using FLUENT V15.0 software and based on the k-ε turbulence model, and treated the behaviour of the multiphase fluid with an Eulerian/Eulerian approach (Singhal et al., 2002). The basic two-phase cavitation model has also been added, which consists of using the conventional mixture transport equations. The helical propagation of the fluid was evidenced, consisting in the circular movement in the (x-y) plane and quasi-linear one along the z-axis with a period ~1 cm close to the outlet tube entrance (z=0). Moreover, due to the friction phenomena, the circular velocity slowly decreased, which results in the period elongation which was experimentally confirmed. This helical movement explains the intensity variations in Figure 2. In fact, the laser beam does not cover the entire (x-y) cross-section area of the tube; therefore the scattered light signal was received from the closest and furthest regions, while the neighbour left and right regions escaped observation. The maximum scattered light intensity therefore was obtained in positions 1, 2, 3 etc. along z-axis, as shown in Figure 3c, where flow lines of the biphasic vapour-liquid fluid approached the receiving optical fiber displaced.

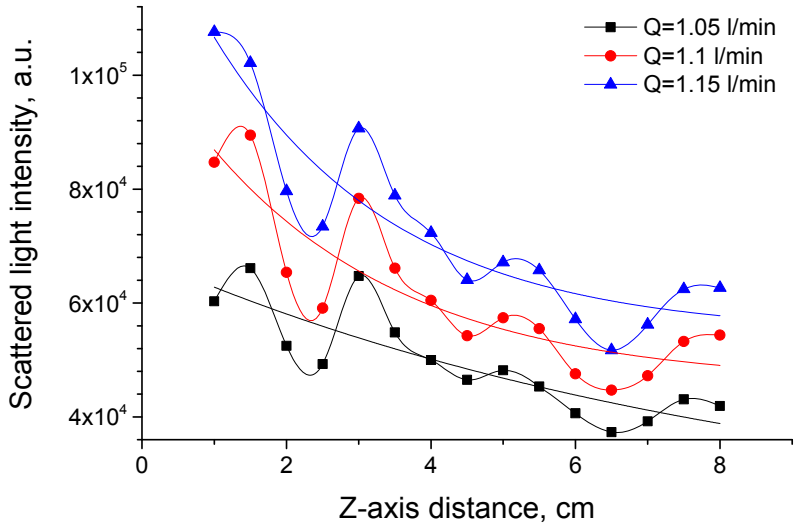

Figure 2: Evolution of scattered light intensity in outlet tube of T-mixer (z-axis) for different flow rates Q above the cavitation threshold (Q^*=0.75 l/min).

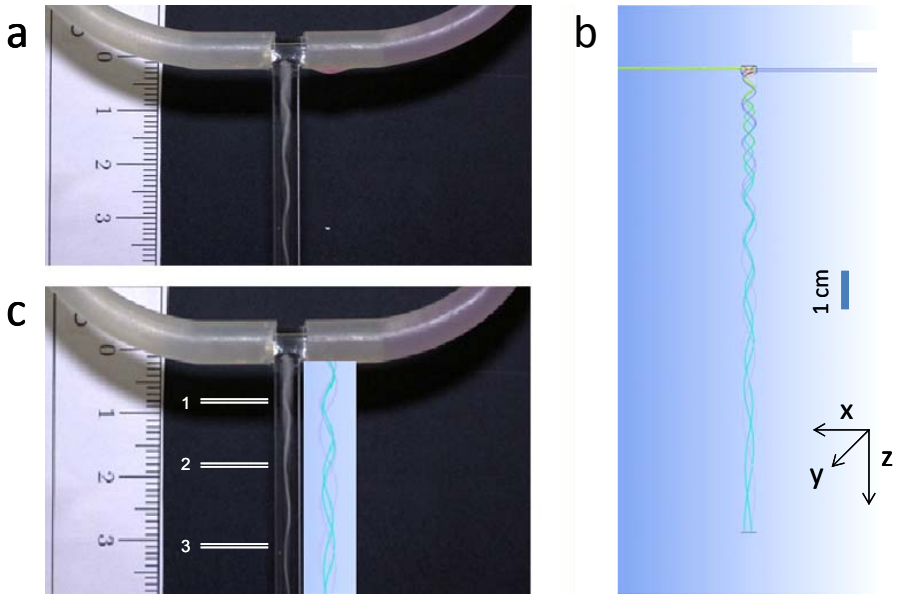

Figure 3: Helical fluid trajectories in T-mixer experimentally observed (a) and calculated (b). Positions of the receiving fiber, corresponding to intensity maxima in Figure 2, are depicted by 1, 2 and 3 in (c).

The DLS method was applied to measurements of a mean apparent size (2R) of the cavitation bubbles.
As it has been previously shown (Rivallin et al., 2003; Rivallin et al., 2005), in agitated media the Stokes-Einstein equation can still be applied to the particle size measurements by replacing the diffusion coefficient due to Brownian thermal motion D_B by the sum of D_B+D_{AG}, where D_{AG} represents particles movement due to the mechanical agitation:

$$R_{app}=k_BT/6\pi\eta(D_B+D_{AG}) \quad (2)$$

Where η is the dynamic viscosity of the fluid and D_{AG} is related to the local specific power input ε:

$$D_{AG}=\lambda(\varepsilon / \nu)^{1/2} \quad (3)$$

Where λ is a constant and ν is kinematic viscosity of the carrying fluid.
According to Eq. (2), the measurements in our agitated fluid with a strong energy input provide an apparent radius R_{app} that underestimates the real radius of the cavitation bubbles.
As shown in Figure 4 for different distances along z-axis of the T-mixer. According to these measurements, the size of the bubbles in the zone of nucleation (z≤1 cm) is about 2R=450 nm (Oualha et al., 2017b) and it steeply decreases to 20 nm at z=2 cm and then slowly grows at longer z up to ~100 nm at z=8 cm.

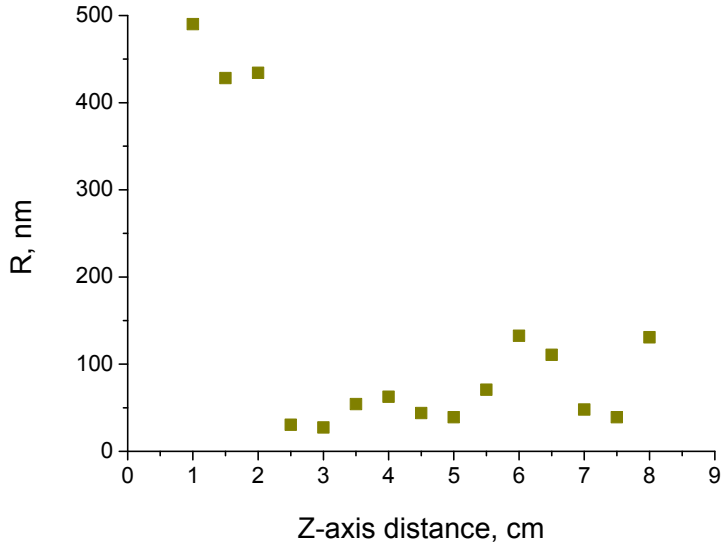

Figure 4: Mean radius of cavitation bubbles along z-axis of outlet tube of T-mixer

To validate these measurements, the size distribution of cavitation bubbles was numerically calculated at different distances of z-axis as shown in Figure 5.

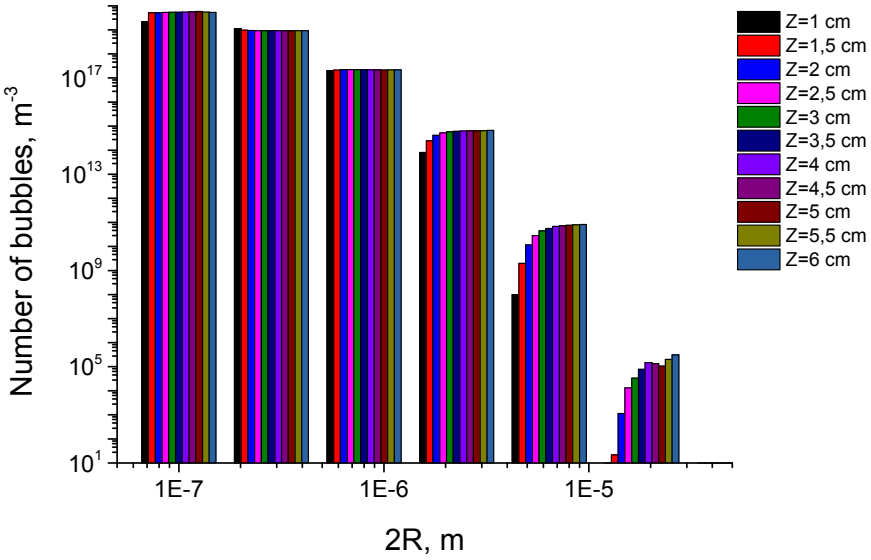

Figure 5: Concentration of bubbles with different sizes (2R) along z-axis of T-mixer (p=7 bar).

In these calculations, cavitation bubbles of different diameters ranging to very small to tens of microns nucleate at the inlet fluids contact in the T-mixer. We consider here physically relevant sizes 2R≥200 nm,

which are beyond the Rayleigh domain ($R<<\lambda$) and significantly contribute to the scattering light intensity. The contributions of different classes of bubbles depend on their surface area of each class (σ)

$$I_{scatt}(R) \propto \sigma = S \times N = 4\pi R^2 \cdot N(R) \quad (4)$$

Despite a broad range of sizes of the cavitation bubbles, the calculated surface area (S) shown in Figure 6 indicates that the major contribution of sizes is between 0.1 and 1 μm, which is in a general agreement with the measured apparent sizes $2R_{app}$ (see Figure 4 and Equation 2) at small z-axis distances, but significantly exceeds sizes measured at longer distances z>2 cm. This may indicate an unusually weak perturbation of DLS measurements in the bubbles generation zone filled with the biphasic vapour-liquid fluid, which understanding requires further studies. On the other hand, much smaller bubbles $R<<R^*$ measured at z>2 cm correspond to an expected perturbation of DLS measurements due to the dissipation of turbulent energy. The following increase of the apparent radius R_{app} (from 50 nm to 100 nm) of the cavitation bubbles with z-axis distance can be explained by the decrease of D_{AG} (Equations 2 and 3), connected to the dissipated energy ε decrease with z, confirmed in our numerical simulations.

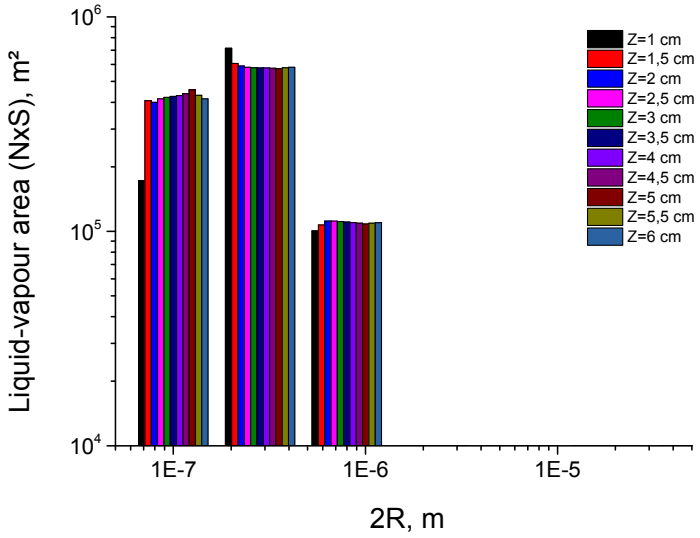

Figure 6: Liquid-vapour area of bubbles with different sizes (2R) along z-axis (p=7 bar)

Conclusions

In this work, the cavitation bubbles kinetics (trajectory, size and number density evolution along the outlet leg of our exocentric T-mixer) in water were studied experimentally by light scattering SLS/DLS measurements and numerically using FLUENT software including the cavitation and population balance models. The appearance of the biphasic (vapour-liquid) fluid at the water injection with $Re>R^*$=8000 enabled light scattering from the fluid. An oscillatory character of the biphasic fluid flow in the outlet tube was observed experimentally and numerically validated, which consisted in the circular movement in the (x-y) plane and quasi-linear propagation along the z-axis. The simulation indicated an appearance of the cavitation bubbles with the most abundant sizes between 0.1 and 1 μm. In contrast, DLS measurements showed the mean apparent radius of the bubbles R_{app}~450 nm close to the zone of the biphasic fluid generation, which steeply decreases down to ~20 nm beyond this zone and subsequently grows at longer distances. The understanding of this behaviour, which is seemingly connected to local changes of the dissipated turbulent energy, needs further studies.
This study contributes to the development of biphasic chemical reactors for nanomaterials elaboration.

References

ANSYS Fluent Population Balance Module Manual, V.15.0, November 2013.

Azouani R., Michau A., Hassouni K., Chhor K., Bocquet J.-F., Vignes J.L., Kanaev A., 2010, Elaboration of pure and doped TiO2 nanoparticles in sol-gel reactor with turbulent micromixing: application to nanocoatings and photocatalysis, Chem. Eng. Res. Des., 88, 1123-1130.

Azouani R., 2009, Elaboration de nouveaux nanomatériaux photocatalytiques actifs sous rayonnement visible, PhD Thesis, Université Paris 13, Villetaneuse, France.

Brennen C. E.,1995, Cavitation and Bubble Dynamics, Oxford University Press.

Cerruti S., Omar M.K., Katz J., 2000, Numerical study of cavitation inception in the near field of an axisymmetric jet at high Reynolds number, Phys. Fluids, 12(10), 2444-2460.

Crowley T.J., Meadows E.S., Evangelos K., Doyle F.J., 2000, Control of particle size distribution described by a population balance model of semibatch emulsion polymerization, J. Process Control, 10, 419-432.

Daniels F., Alberty R.A., 1955, Physical Chemistry, John Wiley and sons, New York.

Kotoulas C., Kiparissides C., 2005, A generalized population balance model for the prediction of particle size distribution in suspension polymerization reactors, Chem. Eng. Sci., 61, 332-346.

Dular M., Griessler-Bulc T., Gutierrez-Aguirre I., Heath E., Kosjek T., Krivograd Klemenčič A., Oder M., Petkovšek M., Rački N., Ravnikar M., Šarc A., Širok B., Zupanc M., Žitnik M., Kompare B., 2016, Use of hydrodynamic cavitation in (waste)water treatment, Ultrasonics Sonochemistry, 29, 577-588.

Fernandez L., 2009, Modélisation par CFD de la précipitation du carbonate de baryum en réacteur à lit fluidisé, PhD Thesis, INPL Nancy-université, France.

Hounslow M. J., Ryall R. L., Marshall V. R., 1988, Discretized Population Balance for Nucleation, Growth and Aggregation, AIChE J, 34, 1821-1832.

Huisman S.G., van Gils D.P.M., Sun C., 2012, Applying laser Doppler anemometry inside a Taylor–Couette geometry using a ray-tracer to correct for curvature effects, Europ. J. of Mech. B/Fluids, 36, 115-119.

Jyoti K.K., Pandit A.B., 2004, Ozone and cavitation for water disinfection, Bioch. Eng. J., 18, 9-19.

Litster J. D., Smit D. J., Hounslow M. J., 1995, Adjustable Discretization Population Balance for Growth and aggregation, AIChE J, 41, 591-603.

Lauterborn W., Bolle H., 1975, Experimental investigations of cavitation-bubble collapse in the neighbourhood of a solid boundary, Jour. Fluid Mech., 72, 391-399.

Liu X., Doub W.H., Guo C., 2010, Evaluation of droplet velocity and size from nasal spray devices using phase Doppler anemometry (PDA), International Journal of Pharmaceutics, 388, 82-87.

Marchisio, Daniele L., Barresi A. A., Baldi G., Rodney F., 2002, Comparison between the classes method and the quadtrature method of moments for multiphase flow, 8th conference : Multiphase flow in industrial plants, Alba, Italy.

Oualha K., Ben Amar M., Michau A., Kanaev A., 2017a, Cavitation Phenomenon in T-mixer with Exocentric Inputs, Chem. Eng. Trans., 57, 1231-1236.

Oualha K., Ben Amar M., Michau A., Kanaev A., 2017b, Observation of cavitation in exocentric T-mixer, Chem. Eng. J., 321, 146–150.

Ramkrishna D., 2000, Population balance, Academic press, London.

Rivallin M., Gaunand A., Kanaev A., 2003, Light Scattering For Sub-Micronic Particle Size measurements in Agitated Suspensions, Chem. Eng. Trans. 3, 919-824.

Rivallin M., Benmami M., Kanaev A., Gaunand A., 2005, Sol-gel reactor with rapid micromixing: modelling and measurements of titanium oxide nano-particles growth, Chem. Eng. Res. Des., 83 (A1), 67-74.

Shokri R., Ghaemi S., Nobes D.S., Sanders R.S., 2017, Investigation of particle-laden turbulent pipe flow at high-Reynolds-number using particle image/tracking velocimetry (PIV/PTV), Int. J. of Multiphase Flow, 89, 136-149.

Singhal A.K., Li H.Y., Athavale M.M., Jiang Y., 2001, Mathematical Basis and Validation of the Full Cavitation Model". ASME FEDSM'01. New Orleans, Louisiana.

Singhal A.K., Athavale M.M., Huiying L., Jiang L., 2002, Mathematical bases and validation of the full cavitation model, J Fluids Eng., 124, 617-623.

Ye X., Yao X., Han R., 2015, Dynamics of cavitation bubbles in acoustic field near the rigid wall, Ocean Eng, 109, 507-516.

Xiong Y., Peng F., 2015, Optimization of cavitation venturi tube design for pico and nano bubbles generation, International Journal of Mining Science and Technology, 25, 523-529.